Effect of Exfoliation and Dispersion on the Yield Behavior of Melt-Compounded Polyethylene–Montmorillonite Nanocomposites

Rowan W. Truss, Tay Kiah Yeow

Division of Materials, School of Engineering, University of Queensland, Brisbane, Queensland, 4072 Australia

Received 27 July 2004; accepted 19 October 2005
DOI 10.1002/app.23703
Published online in Wiley InterScience (www.interscience.wiley.com).

ABSTRACT: The yield behavior of melt-mixed nanocomposites containing 5 wt % organically modified montmorillonite in matrices of a linear low-density polyethylene (LLDPE) or a modified polyethylene was studied as a function of the temperature and strain rate. In the melt-mixed LLDPE nanocomposite, the montmorillonite showed a slight increase in the clay spacing, which suggested that the clay was at best intercalated. Transmission electron microscopy (TEM) images showed that the dispersion in this nanocomposite was poor. The use of the modified polyethylene promoted exfoliation of the clay tactoids in the nanocomposite, as assessed by X-ray diffraction and TEM. In both nanocomposites, the yield mechanisms were insensitive to the addition of the organoclay, even though modest increases in the modulus were produced. © 2006 Wiley Periodicals, Inc. J Appl Polym Sci 100: 3044–3049, 2006

Key words: nanocomposites; polyethylene (PE); yielding

INTRODUCTION

We recently reported some preliminary work on the yield behavior of a melt-mixed linear low-density polyethylene (LLDPE) montmorillonite nanocomposite that showed that the addition of a nanoparticle filler had little effect on the yield behavior.[1] Both the filled and unfilled LLDPE materials showed double yield behavior, and the magnitude of the yield stress was not significantly affected by the addition of the nanoparticle clay up to a 5 wt % loading of the organoclay. Moreover, the mechanisms involved in the double yield points had the same activation energies and were consequently considered to be unaffected by the presence of the filler. Double-yield-point behavior in LLDPE has been studied by numerous workers.[2–8] The activation energies of the two yield processes in the previous work were consistent with the model of Gaucher-Miri and Seguela,[6] in which the low strain yield point is considered to occur by heterogeneous slip between mosaic blocks in the crystallites, whereas the second yield point, leading to necking, results from *c*-axis slip.

The reason that the organoclay filler had little effect on the yield behavior in the previous work on LLDPE nanocomposites may have been the structure of the clay. The melt-mixed nanocomposite was at best intercalated and may have been there as unexfoliated microfiller particles. This would allow the polyethylene to behave somewhat independently of the filler addition. Other works on melt-mixed polyethylene and other nanocomposites based on nonpolar polymers have confirmed the poor dispersion of the clay and lack of exfoliation of the clay in these systems.[9–11]

Recent work on polypropylene- and polyethylene-based nanocomposites have shown that the use of modified resins, which incorporate a polar group, are more successful at generating exfoliated structures in these nonpolar olefins.[12–19] Wang et al.[14] found that exfoliation of the clay in nanocomposites based on LLDPE was promoted when the organic modifier on the clay had more than 16 methyl groups and the maleation level was higher than 0.1 wt %. Osman et al.[15] conducted studies on high-density polyethylene nanocomposites and suggested that complete coverage of the surface of the clay by the surfactant leading to high *d*-spacings also favored exfoliation. Hotta and Paul[16] also found better dispersion in nanocomposites of LLDPE with surfactants with two alkyl tails rather than with surfactants with a single alkyl tail because of the larger *d*-spacing in the clay caused by the bulkier surfactant. Several other studies also indicated the beneficial effect of maleated polyethylene and polypropylene on the exfoliation of the clay in polyethylenes.[17–19]

In many of the previous studies on polyethylene nanocomposites, tensile testing at a single strain rate and temperature has been reported to indicate the effect of the nanocomposite addition on the mechanical properties.[15–17,19] This work describes a systematic

Correspondence to: R. W. Truss (r.truss@uq.edu.au).

study of the yield behavior of a polyethylene-based nanocomposite system in which a modified polyethylene matrix was used to promote exfoliation of the organoclay. This allowed a comparison of the yield behavior between this system and a second system based on unmodified LLDPE in which the clay was at best intercalated with the matrix LLDPE.

The yield behavior was tested in tension, and the yield stress (σ_y) was analyzed as an activated rate process with the Eyring equation:

$$\dot{\varepsilon} = \dot{\varepsilon}_0 \exp - \left(\frac{\Delta H - \sigma_y \nu}{kT}\right) \quad (1)$$

where $\dot{\varepsilon}$ is the strain rate, T is the absolute temperature, ΔH is the activation energy, ν is the activation volume, $\dot{\varepsilon}_0$ is a constant, and k is Boltzmann's constant.

EXPERIMENTAL

Materials

The base polymers used in these experiments were an LLDPE (rotational molding grade; Alkatuff 711UV, Qenos Pty., Ltd., Melbourne, Australia) and a modified polyethylene (maleic anhydride modified LLDPE; Polybond 3109, Uniroyal Chemicals Ptd. Ltd., Melbourne, Australia). The LLDPE had a nominal density of 0.939 g/cm^3 and a melt index of 3.5 g/10 min (ASTM D 1238, 190°C, 2.16 kg). The modified polyethylene had a nominal density of 0.926 g/cm^3, a melt flow rate of 30 g/10 min (ASTM D 1238, 190°C, 2.16 kg), and a nominal maleic anhydride level of 1.0 wt %. The base polymer was compounded with an organically modified montmorillonite clay, Cloisite 15A, supplied by Southern Clay Products, Gonzales, TX, at a rate of 5 wt % Cloisite 15A. The modifier of the natural montmorillonite was a quaternary ammonium salt based on hydrogenated tallow predominantly in the C14–C18 range. The matrix polymer pellets were cryogenically ground and mixed with the powdered clay in the appropriate weight ratio, and this mixture was then compounded with a Eurolab Prism 16-mm twin-screw extruder. The extrudate from the extruder was pelletized and then compression-molded into sheets, ~1.5 mm thick, at a temperature of 210°C and for a pressing time of 3 min. The sheets were cooled in the compression mold, which was internally cooled with circulating water. Tensile samples were cut from the sheet with a dumbbell cutter die made to ASTM D 638 standards (type M-III) with a gauge width of 2.5 mm and a gauge length of 15 mm.

Characterization

The structure of the clay was characterized with both X-ray diffraction (XRD) and transmission electron microscopy (TEM). XRD was carried out on a Bunker AXS discovery X-ray generator in the diffraction mode with an incident X-ray wavelength of 1.540 nm at a scanning rate of 0.5°/min.

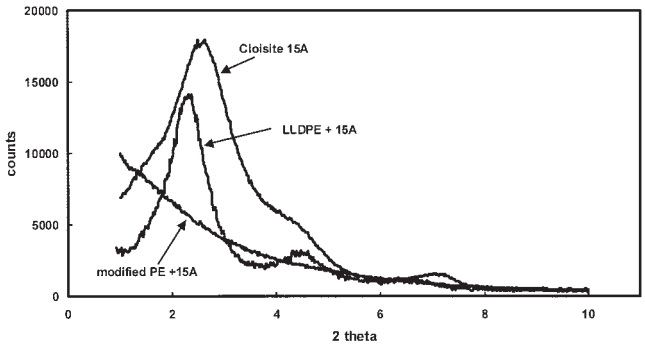

Figure 1 XRD traces at low values of 2θ for Cloisite 15A and nanocomposites based on LLDPE and modified polyethylene (PE) containing 5 wt % Cloisite 15A.

Samples for TEM were sectioned from the pressed sheet with a Leica cryo-ultramicrotome. The microtome was cooled to between −40 and −60°C to make the nanocomposite more rigid for ultrathin sectioning. Thin sections were cut with a dry diamond knife (Diatome, Biel, Switzerland) at a thickness setting of approximately 100 nm. Dry sections were collected on uncoated 700-mesh copper grids and allowed to come to room temperature before being inserted into the TEM instrument. Electron micrograph images were taken on a Tecnai 12 electron microscope (FEI/Veeco, Acht, Holland) operating at 100 keV.

Differential scanning calorimetry (DSC) was conducted with a TA Instruments DSC 2920 at a scanning rate of 10°C/min.

Tensile testing

Tensile tests were conducted on an Instron 4504, High Wycombe, UK, screw-driven tensile testing machine at strain rates from 5.6×10^{-5} to 0.56 s^{-1} and at temperatures of 23–80°C. A constant temperature was achieved with a fan-forced insulated oven fitted to the Instron. For tests conducted at elevated temperatures, the test pieces were held at a temperature for at least 30 min to ensure equilibration of the specimens. Tests were conducted in triplicate.

RESULTS

Characterization

Figure 1 shows the XRD trace for Cloisite 15A and the nanocomposites based on LLDPE and the modified polyethylene containing 5 wt % Cloisite 15A. The XRD trace of the Cloisite 15A clay gave a layer spacing of 32.7 Å. In the LLDPE material, the peak spacing had

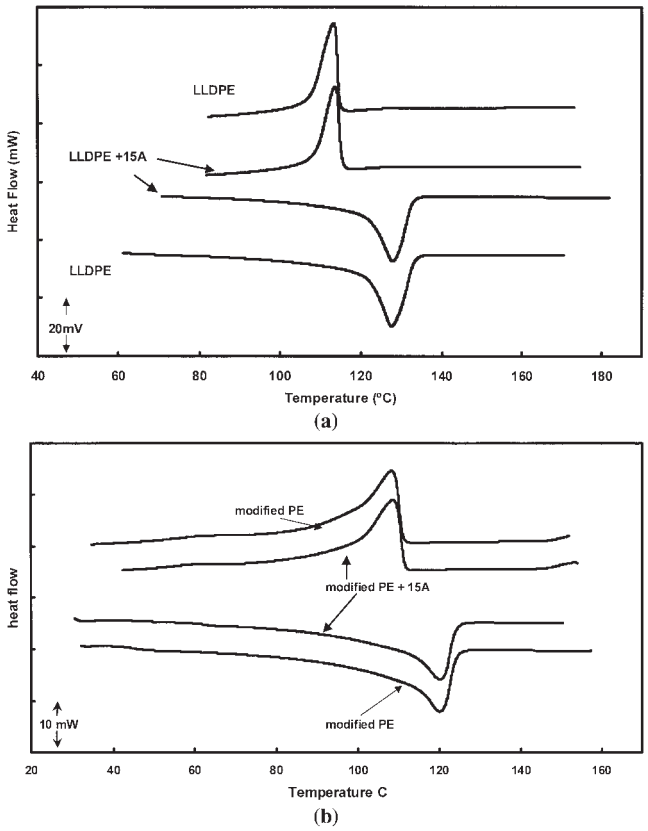

Figure 2 DSC traces for the materials used: (a) LLDPE with and without 5 wt % Cloisite 15 A and (b) modified polyethylene (PE) with and without 5 wt % Cloisite 15 A.

moved to a slightly lower value of 2θ, which corresponded to a layer spacing of 37.1 Å. This was a small increase in the clay layer spacing in the nanocomposite and suggested an intercalated structure. Upon the compounding of the clay into the modified polyethylene, a peak due to the clay layer spacing was no longer detected in the XRD trace. Although other factors such as the size, concentration, and orientation of the remaining tactoids may limit the detectability of the clay layer spacing, the diffraction trace did indicate a significant disruption of the clay tactoids. TEM analysis of microtomed sections of this material confirmed that the clay had been largely exfoliated, although some distorted tactoids may still have been present. This morphology contrasted with the melt-mixed LLDPE-based nanocomposite, which clearly showed individual clay tactoids within the structure. In this material, the distribution of the clay particles appeared reasonably uniform, but the dispersion of the clay platelets was poor.

Figure 2 shows DSC traces for both matrix polymers and the nanocomposites containing 5 wt % organoclay. The traces showed that both the position and magnitude of the melting enthalpy peak were not significantly changed upon the addition of the nanoclay material to the matrix polyethylene, indicating that there was no significant change in the crystallinity of the samples with the addition of the clay. In addition, there was little discernable difference in the crystallization peak on cooling, and this suggested that the clay did not act as a strong nucleating agent for the polyethylene. The modified polyethylene did show a lower melting temperature and a more diffuse melting region than the unmodified LLDPE. It was difficult to measure the melting enthalpy in the modified polyethylene accurately because the DSC trace showed a very gradual change in the slope on melting. However, the crystallinity in the modified polyethylene materials was significantly lower (25–30% lower) than that of the LLDPE materials. This was to be expected because the presence of grafted groups on the molecule would interfere with the crystallization of the polyethylene.

Tensile testing

Figure 3(a) shows typical stress–strain curves for the LLDPE with and without the addition of 5 wt % Cloisite 15A, whereas Figure 3(b) presents similar plots for the modified polyethylene. Little difference was observed between the shapes of the curves for the filled and unfilled materials in both systems. Two events were observed during the yield and drawing of

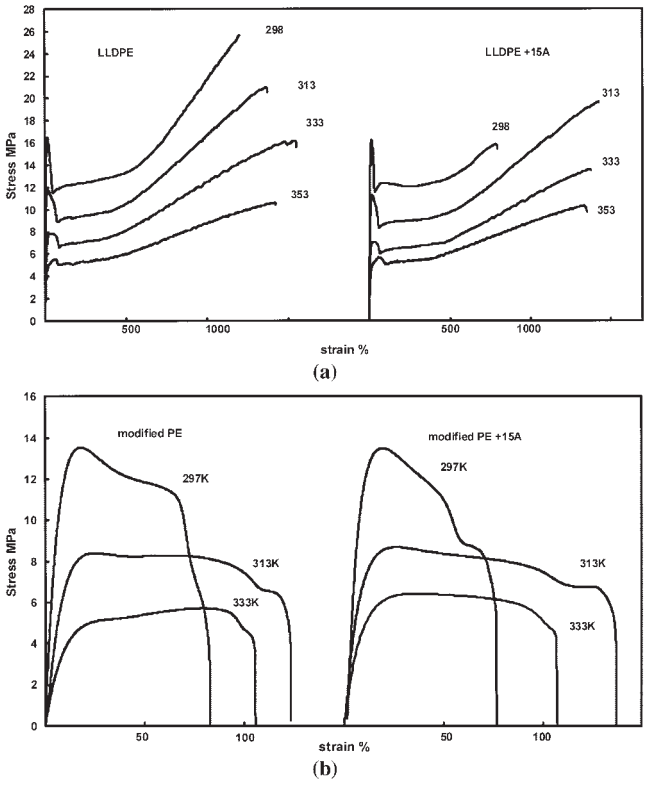

Figure 3 Typical stress–strain curves at different temperatures for (a) LLDPE and (b) modified polyethylene (PE) with and without the addition of 5 wt % Cloisite 15A.

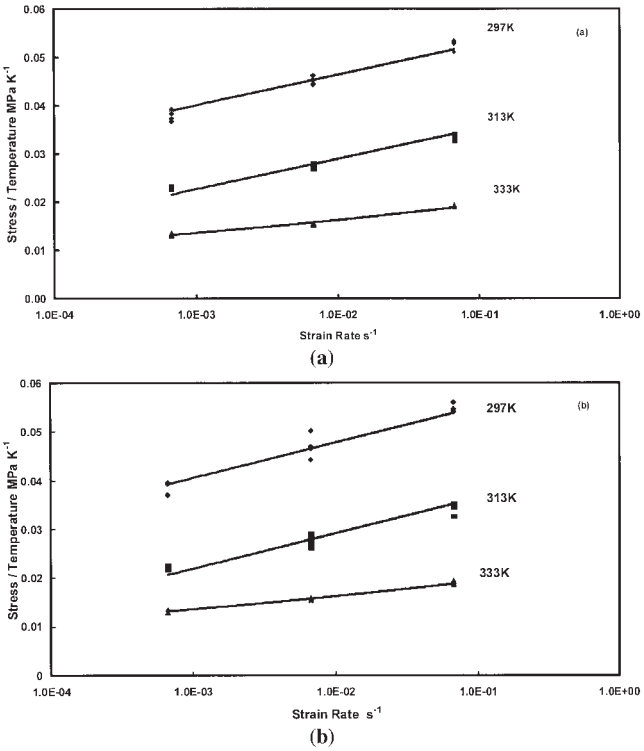

Figure 4 Eyring plots for the first yield point: (a) modified polyethylene matrix and (b) the matrix and 5 wt % organoclay.

these materials. An event occurred at a low strain of 15–20% that was followed by a second event at much higher strains of ~60–100%, at which an inhomogeneous neck formed. At high temperatures and low strain rates, the stress at the first yield point was lower than that at the second yield point, but at lower temperatures and higher strain rates, the stress at the second yield point was lower than that of the first. In the LLDPE materials, the neck once formed was stable, and the drawing of the whole gauge length occurred so that strains at break were several hundred percent. However, in the modified polyethylene materials, the neck once formed did not propagate down the gauge length, but final failure of the specimen occurred soon after the formation of the neck. This resulted in much lower strains to failure in the modified polyethylene materials in comparison with the unmodified LLDPE samples.

Figure 4 shows the strain rate and temperature dependence for the first yield event for the base modified polyethylene material [Fig. 4(a)] and the modified polyethylene nanocomposite [Fig. 4(b)]. These data are plotted in accordance with eq. (1). Similar plots were obtained for the LLDPE and LLDPE-based nanocomposite. Parallel straight lines were obtained at low temperatures, but a deviation from this trend occurred at higher temperatures and low strain rates. For the modified polyethylenes, the deviation from the single Eyring process behavior occurred at a test temperature of 60°C, whereas for the LLDPE materials, the deviation occurred at a higher temperature of ~80°C. Equation (1) was fitted to the data obtained at lower test temperatures, at which the data formed parallel straight lines, and the best fit parameters to the Eyring constants are listed in Table I.

Figure 5 shows the strain rate and temperature dependence of the second yield point for the modified polyethylene materials. The second yield point was associated with nonhomogeneous deformation and the formation of a distinct neck in the specimen. Again, these data formed parallel straight lines at the lower temperatures but deviated from this behavior at higher temperatures. The lower temperature data were again fitted to eq. (1), and the fitting parameters are listed in Table I. Similar results for the LLDPE materials are also shown in Table I.

DISCUSSION

The addition of the organoclay had little effect on the yield behavior of either the LLDPE-based materials or the modified polyethylene materials. The major differences observed in the systems studied here were the distinctly lower yield stress measured for the modified polyethylene materials and the fact that the inhomogeneous neck when formed at the second yield point was stable and propagated down the gauge length in the LLDPE materials, but necking was followed closely by final failure in the modified polyethylene materials.

TABLE I
Best Fit Eyring Parameters for the Two Yield Points for the Different Materials

Material	Yield (I)			Yield (II)		
	ΔH (kJ/mol)	ν (Å^3)	ln $\dot{\varepsilon}_0$	ΔH (kJ/mol)	ν (Å^3)	In $\dot{\varepsilon}_0$
LLDPE	235	5,238	70.5	313	11,173	89.7
LLDPE + 5 wt % Cloisite 15A	221	5,139	66.0	316	11,810	90.8
Modified polyethylene	329	5,040	111	391	9,510	127
Modified polyethylene + 5 wt % Cloisite 15A	305	4,370	103	439	8,500	149

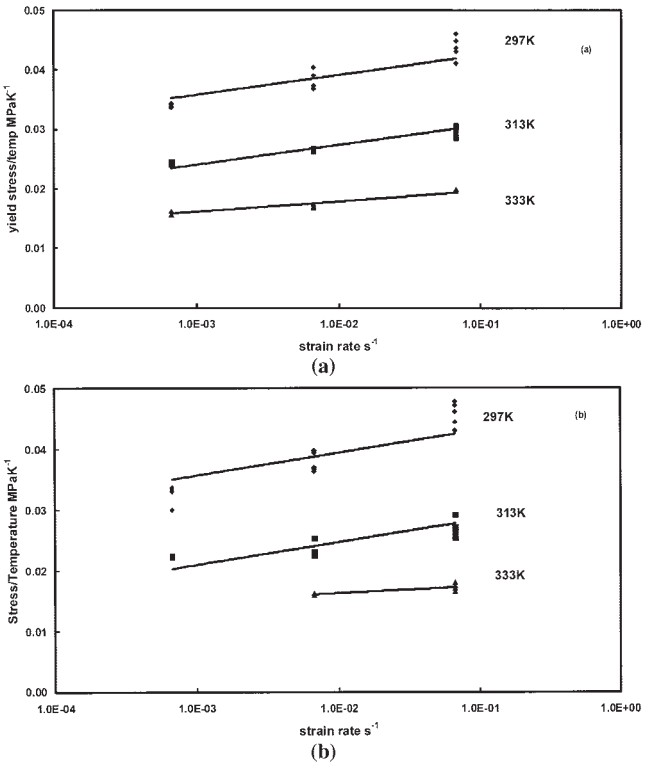

Figure 5 Eyring plots for the second yield point: (a) modified polyethylene matrix and (b) the matrix and 5 wt % organoclay.

Double-yield-point behavior was observed in both the filled and unfilled materials. At low temperatures and high strain rates, the lower strain yield point occurred at the higher stress of the two yield events. The second yield point occurred at a higher stress than the first yield point at low strain rates and high temperatures. This change in behavior resulted from the different strain rate dependences of the two yield events in these materials. Double-yield-point behavior in LLDPE has been studied by numerous workers.[2–8] The activation energies of the two yield processes in the LLDPE materials were consistent with the model of Gaucher-Miri and Seguela,[6] in which the low strain yield point is considered to occur by heterogeneous slip between mosaic blocks in the crystallites, whereas the second yield point, leading to necking, results from *c*-axis slip.

The key finding here was that the activation energies for the first yield point in the filled polyethylenes were unchanged from those obtained for the base polymer. However, in the case of the modified polyethylene, the activation energy for the first yield point, ~300 kJ/mol, was higher than that for the LLDPE samples, ~220 kJ/mol. The second yield process in the modified polyethylene samples also had a higher activation energy, ~400 kJ/mol, than that of the LLDPE samples, ~320 kJ/mol.

The value for the activation energy for the first yield point in the modified polyethylene, ~300 kJ/mol, was similar to the value of the activation energy for the second yield process in LLDPE, ~320 kJ/mol, and there is a temptation to equate the mechanisms involved. The second yield point in the LLDPE materials was considered to be associated with *c*-axis slip and necking in the sample. However, at the first yield point in the modified polyethylenes, the strain was not localized into a neck. Moreover, the strains for the yield processes in both sets of materials were similar, and thus it would appear more likely that the yield mechanisms had not changed with the modification of the polyethylene but that the presence of the maleic anhydride groups had increased the activation energy for the deformation processes. The presence of these groups might be expected to increase the stiffness of the molecular chain and interrupt the crystallinity of the polyethylene. The latter would be the cause of the overall lower yield stresses in the modified polyethylene materials, whereas the former could be expected to affect the temperature dependence of the materials from which the activation energy is calculated.

The fact that there was little difference in the yield behavior with the addition of the organoclay to the LLDPE was understandable in light of the structure of the composite. The DSC results showed that there did not appear to be a significant change in the crystallinity of the LLDPE with the addition of the organoclay. More importantly, although the XRD suggested that an intercalated structure might have formed, TEM clearly showed that the filler was there as discrete particles. Consequently, the material most likely behaved as a conventional microcomposite, and the filler particles did not interrupt the normal deformation mechanism associated with the yield of the semicrystalline structure. Little change in the magnitude of the yield stresses was observed due to the presence of the filler particles because their volume fraction was quite small.

It was more surprising that the yield behavior of the nanocomposite based on the modified polyethylene was also not affected by the presence of the organoclay. The XRD pattern for this material showed no peak at a low 2θ value that would correspond to the clay *d*-spacing. This suggested that the clay had been significantly exfoliated, and this was supported by the TEM micrographs. If the yield of the polyethylene involved slip between mosaic blocks and *c*-axis slip, then the key structural feature in the matrix polyethylene would be the lamellae, which are 10–20 nm thick and much larger in their lateral dimensions. These lamellae can be incorporated into spherulites of micrometer and higher dimensions. Although the clay platelets are nanometers thick, their lateral dimensions are microscale. Thus, exfoliated clay platelets might be expected to disrupt the microstructure of the

polyethylene matrix and consequently might also be expected to affect the yield mechanisms. However, this did not occur in the modified polyethylene materials. The DSC results for the maleic anhydride grafted material gave a broad melting range starting at quite low temperatures, suggesting that the crystalline microstructure had already been disrupted by the presence of the grafted groups in the matrix polymer. Further alteration of the microstructure due to the introduction of the clay platelets may then be insignificant in terms of controlling the deformation mechanisms of the polymer.

Figures 4 and 5 show the stress at the first and second yield events for the different materials as a function of the strain rate and temperature, plotted in accordance with eq. (1). Parallel straight lines were obtained at lower temperatures, but a deviation from this trend occurred at ~60°C for the modified polyethylene materials and at ~80°C for the LLDPE samples. The DSC curves (Fig. 2) show that the presence of the maleic anhydride groups on the polyethylene reduced the temperature for the onset of melting and broadened the temperature range over which the melting process occurred. This lowering of the melting point correlated with the temperature at which the yield data deviated from the single-process Eyring-type behavior [eq. (1)]. Thus, the deviation of the yield data at higher temperatures and lower strain rates may be associated with the onset of melting in the samples or possibly the ability of the materials to recrystallize during testing.

Both the filled and unfilled modified polyethylene materials were unable to form a stable neck. For a stable neck to form, work hardening of the drawing material needed to occur. The modified materials used in this work had a high melt flow index, which probably reflected a low molecular weight. The low molecular weight limited the number of entanglements that formed, and consequently the neck, once formed, had limited ability to work-harden and drew to a point and failed. Rotation of mosaic blocks in the crystallites should not be greatly affected by the molecular weight, but the ability to orient the polymer between entanglements when *c*-axis slip occurs would be expected to be dependent on the molecular weight. This also suggests that the molecular mechanism involved in the second yield process in the modified materials was *c*-axis slip similar to the mechanism found in the unmodified LLDPE.

CONCLUSIONS

The addition of an organoclay to both an LLDPE and a maleic anhydride grafted polyethylene had little effect on the yield behavior of the base polymers. This was true even though melt mixing of the organoclay into the LLDPE resulted in an intercalated but poorly dispersed composite, whereas compounding the organoclay into the modified polyethylene resulted in significant exfoliation of the clay. In both systems, the unfilled and filled materials showed double-yield-point behavior. An analysis of the yield behavior with an Eyring-type approach showed that the activation energies for the yield events were unchanged by the addition of the nanoscale filler. Moreover, the yield mechanisms appeared to be the same in the modified polyethylene materials as those found for LLDPE intercalated nanocomposites.

The assistance of Kayleen Campbell in obtaining the transmission electron micrographs and Ang Chiean Lee for data on the LLDPE materials is gratefully acknowledged.

References

1. Truss, R. W.; Lee, A. C. Polym Int 2003, 52, 1790.
2. Popli, R.; Mandelkern, L. J Polym Sci Part B: Polym Phys 1987, 25, 4412.
3. Segeula, R.; Rietsch, F. J Mater Sci Lett 1990, 9, 46.
4. Brooks, N. W.; Duckett, R. A.; Ward, I. M. Polymer 1992, 3, 1872.
5. Segeula, R.; Darras, O. J Mater Sci 1994, 29, 5342.
6. Gaucher-Miri, V.; Segeula, R. Macromolecules 1997, 30, 1158.
7. Butler, M. F.; Donald, A. M.; Ryan, A. J. Polymer 1997, 38, 5521.
8. Xu, X.-R.; Xu, J.-T.; Feng, L.-X. Polym Int 2002, 51, 458.
9. Jeon, H. G.; Jung, H. T.; Lee, S. W.; Hudson, S. D. Polym Bull 1998, 41, 107.
10. Furuichi, N.; Kurokawa, Y.; Fujita, K.; Oya, A.; Yasuda, H.; Kiso, M. J Mater Sci 1996, 31, 4307.
11. Heinemann, J.; Reichert, P.; Mulhaupt, R. Macromol Rapid Commun 1999, 20, 423.
12. Kawasumi, M.; Hasegawa, N.; Kato, M.; Usuki, A.; Okada, A. Macromolecules 1997, 30, 6333.
13. Liu, X.; Wu, Q. Polymer 2001, 42, 10013.
14. Wang, K. H.; Choi, M. H.; Koo, C. M.; Choi, Y. S.; Chung, I. J. Polymer 2001, 42, 9819.
15. Osman, M. A.; Rupp, J. E. P.; Suter, U. W. Polymer 2005, 46, 1653.
16. Hotta, S.; Paul, D. R. Polymer 2004, 45, 7639.
17. Liang, G.; Xu, J.; Bao, S.; Xu, W. J Appl Polym Sci 2004, 91, 3974.
18. Ranade, A.; Nayak, K.; Fairbrother, D.; D'Souza, N. A. Polymer 2005, 46, 7323.
19. Lee, J.-H.; Jung, D.; Hong, C.-E.; Rhee, K. Y.; Advani, S. G. Comput Sci Technol 2005, 65, 1996.